

RESEARCH ARTICLE | DECEMBER 12 2023

Self-interaction correction schemes for non-collinear spin-density-functional theory

Nicolas Tancogne-Dejean  ; Martin Lüders ; Carsten A. Ullrich 

 Check for updates

J. Chem. Phys. 159, 224110 (2023)

<https://doi.org/10.1063/5.0179087>

 CHORUS



View
Online



Export
Citation

Articles You May Be Interested In

Scaling down the Perdew-Zunger self-interaction correction in many-electron regions

J. Chem. Phys. (March 2006)

The effect of the Perdew-Zunger self-interaction correction to density functionals on the energetics of small molecules

J. Chem. Phys. (September 2012)

Ionization potentials and electron affinities in the Perdew-Zunger self-interaction corrected density-functional theory

J. Chem. Phys. (May 2005)

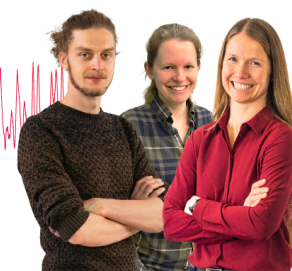
Webinar From Noise to Knowledge

May 13th – Register now



Zurich
Instruments

Universität
Konstanz



Self-interaction correction schemes for non-collinear spin-density-functional theory

Cite as: *J. Chem. Phys.* **159**, 224110 (2023); doi: [10.1063/5.0179087](https://doi.org/10.1063/5.0179087)

Submitted: 29 September 2023 • Accepted: 17 November 2023 •

Published Online: 12 December 2023



View Online



Export Citation



CrossMark

Nicolas Tancogne-Dejean,^{1,2,a)}  Martin Lüders,^{1,b)}  and Carsten A. Ullrich^{3,c)} 

AFFILIATIONS

¹Max Planck Institute for the Structure and Dynamics of Matter and Center for Free-Electron Laser Science, Luruper Chaussee 149, 22761 Hamburg, Germany

²European Theoretical Spectroscopy Facility, www.etsf.eu

³Department of Physics and Astronomy, University of Missouri, Columbia, Missouri 65211, USA

Note: This paper is part of the JCP Festschrift for John Perdew.

^{a)}Author to whom correspondence should be addressed: nicolas.tancogne-dejean@mpsd.mpg.de

^{b)}Electronic mail: martin.lueders@mpsd.mpg.de

^{c)}Electronic mail: ullrichc@missouri.edu

ABSTRACT

We extend some of the well-established self-interaction correction (SIC) schemes of density-functional theory—the Perdew–Zunger SIC and the average-density SIC—to the case of systems with noncollinear magnetism. Our proposed SIC schemes are tested on a set of molecules and metallic clusters in combination with the widely used local spin-density approximation. As expected from the collinear SIC, we show that the averaged-density SIC works well for improving ionization energies but fails to improve more subtle quantities like the dipole moments of polar molecules. We investigate the exchange–correlation magnetic field produced by our extension of the Perdew–Zunger SIC, showing that it is not aligned with the local total magnetization, thus producing an exchange–correlation torque.

© 2023 Author(s). All article content, except where otherwise noted, is licensed under a Creative Commons Attribution (CC BY) license (<http://creativecommons.org/licenses/by/4.0/>). <https://doi.org/10.1063/5.0179087>

I. INTRODUCTION

In practical (spin) density-functional theory (DFT) calculations, one needs to select an approximate functional of the density to compute the exchange–correlation energy and the corresponding potential.¹ Most of the commonly employed approximations are known to suffer from the so-called self-interaction error,² an error that implies that the electron can interact with itself via the total electronic density. The self-interaction error can lead to problems in the prediction of the electronic properties of molecules and materials. For example, it can cause an underestimation of the bandgap of insulators and semiconductors and an underestimation of the ionization potential and electron affinity of molecules. Therefore, correcting for the self-interaction error is important for obtaining reliable DFT predictions of the electronic properties of molecules and materials.³

The search for schemes correcting the self-interaction error, known as self-interaction correction (SIC), has been pioneered by Perdew and Zunger,² even if prior attempts have been made to solve this problem for exchange.⁴ Their proposed method, now referred to

as the Perdew–Zunger self-interaction correction (PZ-SIC), leads to an exchange–correlation energy functional that is an explicit functional of the orbitals and, hence, an implicit density functional. Implementations of the PZ-SIC approach are often performed in a generalized Kohn–Sham sense,⁵ where the exchange–correlation potential depends on the orbital on which it acts. Alternatively, and in the spirit of the original Kohn–Sham DFT, a local multiplicative exchange–correlation potential can be constructed from PZ-SIC using the optimized effective potential (OEP) technique.⁶ The so-constructed exchange–correlation potentials have the correct asymptotic behavior and exhibit discontinuities as a function of particle number.^{3,7}

It is possible to solve the OEP equations exactly,^{8,9} but this is known to be numerically challenging, and one often resorts to the scheme introduced by Krieger, Li, and Iafrate (KLI) to approximate the full solution of the OEP equations.¹⁰ A further simplification of the KLI approach is the Slater approximation, which neglects the orbital-dependent part in the OEP equations and replaces it by an orbital-averaged term.¹⁰ The so-called globally averaged method

(GAM) is defined in a similar spirit.^{11,12} An even more drastic approximation for the SIC consists of replacing in the PZ-SIC the orbital-dependent part directly by an averaged value for all orbitals, leading to the average-density SIC (AD-SIC).¹³ More recently, Zope and co-workers proposed new schemes like the local-scaling SIC,¹⁴ which are intended to fix some of the known deficiencies of the original PZ-SIC; unlike the other methods mentioned earlier, this method is not a simplification of the OEP equation but an alternative to PZ-SIC.

To our knowledge, all of these methods have so far only been proposed and employed in the context of spin DFT (SDFT) with collinear spins, with a notable exception of the perturbative treatment of SIC for noncollinear spin performed in Ref. 15. However, there exist many electronic systems in which noncollinear magnetism, spin-orbit coupling (SOC), and other relativistic effects are relevant, and these are usually treated with the local spin density approximation (LSDA) or with semilocal approximations, which suffer from self-interaction error.

It is the goal of this paper to explore how to extend the applicability of the above-mentioned SIC schemes to the realm of noncollinear magnetism.^{16–18} This allows one to include effects stemming from the noncollinear magnetism and, at the same time, improve upon the LSDA.

Extending the existing SIC schemes to treat noncollinear magnetism requires care. Important fundamental conditions are the local SU(2) gauge invariance of the exchange-correlation energy and the requirement that the method properly reduces to the collinear limit. Moreover, an important question is whether the exchange-correlation magnetic field produced by a noncollinear SIC can exert a local torque on the magnetization.^{19,20} If such a torque exists, it must satisfy the condition that the system cannot exert a global torque on itself (this is known as the zero-torque theorem of SDFT).²¹ It is the goal of this work to discuss these points.

The paper is organized as follows. In Sec. II, we present the motivation underlying our proposed SIC and extend the collinear formulation of PZ-SIC and AD-SIC to the noncollinear case. Then, in Sec. III, we report numerical results obtained for several isolated systems, for which we analyze the effect of the SIC on the electronic and magnetic properties of atoms, small molecules, and clusters. We also discuss its effect on the local texture of the exchange-correlation torque. Finally, we draw our conclusions in Sec. IV.

II. THEORY

We begin by defining the concept of self-interaction for the general case of noncollinear spin systems. Self-interaction is usually introduced separately for exchange and correlation. Therefore, let us first consider the exact exchange energy of a system of N electrons,²²

$$E_x[n, \mathbf{m}] = -\frac{1}{2} \iint \frac{d\mathbf{r}d\mathbf{r}'}{|\mathbf{r}-\mathbf{r}'|} \text{Tr} \left[\underline{\underline{\gamma}}(\mathbf{r}, \mathbf{r}') \underline{\underline{\gamma}}(\mathbf{r}', \mathbf{r}) \right], \quad (1)$$

where Tr is the trace over spin indices of the one-particle spin density matrix $\gamma_{\sigma\tau}(\mathbf{r}, \mathbf{r}') = \sum_j^N \psi_{j\sigma}(\mathbf{r}) \psi_{j\tau}^*(\mathbf{r}')$, constructed from two-component spinor orbitals, where $\sigma = \uparrow, \downarrow$, and likewise for τ . Here, the double underline in $\underline{\underline{\gamma}}$ represents a 2×2 matrix in spin space.¹⁸ The charge and magnetization densities, n and \mathbf{m} , are defined as

$$n(\mathbf{r}) = \sum_j^N \sum_{\sigma} \psi_{j\sigma}(\mathbf{r}) \psi_{j\sigma}^*(\mathbf{r}), \quad (2)$$

and

$$\mathbf{m}(\mathbf{r}) = \sum_j^N \psi_j(\mathbf{r}) \boldsymbol{\sigma} \psi_j^*(\mathbf{r}), \quad (3)$$

respectively, where $\boldsymbol{\sigma} = (\sigma_x, \sigma_y, \sigma_z)$ is the vector of the Pauli matrices. The Hartree energy is given by

$$E_H[n] = \frac{1}{2} \iint d\mathbf{r}d\mathbf{r}' \frac{n(\mathbf{r})n(\mathbf{r}')}{|\mathbf{r}-\mathbf{r}'|}, \quad (4)$$

where $n(\mathbf{r}) = \text{Tr}[\underline{\underline{\gamma}}(\mathbf{r}, \mathbf{r})]$ is the total charge density of the system.

From the above-mentioned definitions of E_x and E_H , it is straightforward to show that in the one-electron case, we have

$$E_x[n_i, \mathbf{m}_i] + E_H[n_i] = 0, \quad (5)$$

where n_i and \mathbf{m}_i are the single orbital charge and magnetization densities. This is the generalization of the result shown in Ref. 2 for the collinear case and forms the basis of the self-interaction corrections that we are proposing below.

More generally, for a single orbital, there is no correlation energy, so we can say that the exchange-correlation energy should fulfill the constraint

$$E_{xc}[n_i, \mathbf{m}_i] + E_H[n_i] = 0. \quad (6)$$

Importantly, we remark here that both the exchange energy, Eq. (1), and the Hartree energy, Eq. (4), are invariant under local rotations of the spin. Such a local rotation of the spins is called an SU(2) rotation, and the operation associated with the rotation of the spins is referred to as an SU(2) gauge transformation. If the energy of an electronic system is SU(2) gauge invariant, it means that it is left unchanged by any SU(2) gauge transformation. This is the case for E_x , Eq. (1), and E_H , Eq. (4). We thus obtain from Eq. (6) that the property remains true if we rotate the orbitals such that their magnetization aligns with the z direction,

$$E_{xc}[n_i, \hat{R}_z \mathbf{m}_i] + E_H[n_i] = 0, \quad (7)$$

where $\hat{R}_z \mathbf{m}_i$ is a symbolic operator notation for performing a rotation on the spin parts of all orbitals such that they are reckoned with respect to a given global z -axis and then constructing the resulting orbital magnetizations.

This allows us to make the link with the collinear result [see Eq. (30) of Ref. 2]. Of course, when starting from the noncollinear formulation of SDFT, one needs to break some symmetries to reduce the four-component noncollinear theory based on the variables (n, \mathbf{m}) into a two-component collinear theory based on the variables (n, m_z) . This can be achieved, for instance, using a uniform magnetic field of small magnitude along the z -axis, which causes the orbitals to align their magnetization along this direction. In other words, the system needs to be told to choose the z -axis as its spin quantization axis.

From this, we obtain a set of necessary conditions to be able to employ Eq. (5) to build a SIC. The first condition is that the approximate exchange-correlation functional must be locally SU(2) gauge

invariant, i.e., it produces the same exchange-correlation energy independently of the orientation of the orbital magnetization.

The second condition is that the noncollinear and collinear functionals should produce the same energy at the same density for a magnetization along the z direction. In other words, $E_{xc}^{\text{noncoll.}}[n_i, m_{i,z}\hat{e}_z] = E_{xc}^{\text{coll.}}[n_{i\sigma}, 0]$, where it is stipulated that $m_{i,z} = n_{i,\uparrow} - n_{i,\downarrow}$ and $n_{i,\uparrow} = n_{i,\downarrow} = 0$ (and hence $m_{i,x} = m_{i,y} = 0$). The collinear functional $E_{xc}^{\text{coll.}}[n_{i\sigma}, 0]$ appears in the definition of PZ-SIC (see below).

These conditions are naturally fulfilled by the LSDA when using the method proposed originally by Kübler *et al.*²³ The first condition is also fulfilled by the more recently proposed noncollinear exchange *meta*-GGA,^{22,24} which also properly recovers the result of the Becke–Roussel collinear exchange functional²⁵ for closed-shell systems.

A. Noncollinear Perdew–Zunger SIC

Based on Eq. (5), we can propose a generalization of the PZ-SIC to the noncollinear case. Let us first start by reviewing briefly the collinear case. The idea behind the PZ-SIC consists of removing all the single-electron self-interaction errors for a given density functional approximation. This leads to the energy functional

$$E_{xc}^{\text{SIC}} = E_{xc}^{\text{DFT}}[n_{\uparrow}, n_{\downarrow}] - \sum_{\sigma=\{\uparrow,\downarrow\}} \sum_i f_{i,\sigma} (E_{\text{H}}[n_{i\sigma}] + E_{xc}^{\text{DFT}}[n_{i\sigma}, 0]). \quad (8)$$

In this expression, n_{\uparrow} and n_{\downarrow} refer, respectively, to the up and down channels of the total electronic density, and the $f_{i,\sigma}$ are occupation numbers. For each orbital φ_i , one needs to compute the corresponding Hartree and exchange-correlation energy from its individual density $n_{i\sigma}$ and subtract it from the energy computed from the total density.

This above-mentioned expression is intrinsically limited to the collinear case but can be easily generalized to the noncollinear case. Indeed, in the latter case, the exchange-correlation functional is not a functional of the density in the two spin channels ($E_{xc}[n_{\uparrow}, n_{\downarrow}]$) but a functional of the total density n and the local magnetization \mathbf{m} . This immediately suggests generalizing Eq. (8) to the noncollinear case as

$$E_{xc}^{\text{SIC}} = E_{xc}^{\text{DFT}}[n, \mathbf{m}] - \sum_i f_i (E_{\text{H}}[n_i] + E_{xc}^{\text{DFT}}[n_i, \mathbf{m}_i]). \quad (9)$$

This correction removes the self-interaction of each orbital φ_i , as in the collinear case.

In practice, the noncollinear PZ-SIC scheme can be challenging to implement. First of all, it requires finding the local effective potential originating from this orbital-dependent scheme, unless one wants to resort to using a generalized Kohn–Sham scheme that allows for orbital-dependent potentials.⁵ Finding this local multiplicative potential is usually achieved by solving the OEP equation^{6,8} or some simplified version of it, like the KLI approximation.¹⁰

A more subtle complexity comes from the fact that different orbitals can produce the same density. For a typical density functional approximation like LSDA, this is not a problem. However, this becomes a well-known problem with PZ-SIC, whose results depend on the orbitals and hence vary under a unitary transformation of the orbitals.^{26–30} It was first realized by Perderson and co-workers^{28,29} that certain conditions needed to be fulfilled to minimize the

PZ-SIC energy, referred to as the localization equations. In practice, one needs to explicitly minimize all possible unitary transformations.^{8,31} Alternatively, one can use specific orbitals that make the SIC a true density functional.³² We will briefly discuss this point below with numerical examples.

Finally, let us comment on an important difference between the collinear case and the noncollinear case, which concerns the practical solution of the KLI equations to get to an approximate solution to the full OEP equation. When solving these equations, the potential is defined up to a constant, which is fixed by imposing for isolated systems that $v_{xc,\sigma} \rightarrow 0$ for r going to infinity.¹⁰ This leads to a different constant for the up and down potentials in the collinear case. However, in the noncollinear case, we end up with a single constant, as we have a 2×2 matrix in spin space for the potential. As a consequence, for an open-shell system without SOC, for which we can directly compare the collinear and noncollinear results, the potentials for the majority spin are very similar, but in the minority spin channel, they may be different.

B. Noncollinear averaged density SIC

While the PZ-SIC is known to produce very good results, it is also known to be numerically expensive to evaluate, as one needs to solve one Poisson equation and compute the exchange-correlation energy for each occupied Kohn–Sham state, and one further needs to solve the OEP equations to obtain the local multiplicative potential needed to perform Kohn–Sham SDFT calculations. This is why several simplified methods have been proposed. Among them, the most effective method is probably AD-SIC, which, a bit surprisingly given its simplicity, can produce excellent results for atoms compared to PZ-SIC.³³ The motivation of this method is that if all orbitals have a similar localization, we can replace their density in Eq. (8) by their averaged density.⁸ This is particularly suited for calculations with identical atoms and pseudopotential-based simulations, as orbitals are similar in these cases. However, AD-SIC suffers from a size-consistency problem as it is explicitly based on the number of electrons,⁸ which makes it unsuitable for extended systems. In this section, we show how to generalize the AD-SIC to the noncollinear case.

In the collinear case, the AD-SIC is obtained by replacing in Eq. (8) the orbital and spin-resolved density $n_{i\sigma}$ by the average spin-resolved density n_{σ}/N_{σ} , where $N_{\sigma} = \int dr n_{\sigma}(\mathbf{r})$ is the number of electrons in the spin channel σ . This directly leads to the collinear AD-SIC energy functional,

$$E_{xc}^{\text{AD-SIC}} = E_{xc}^{\text{DFT}}[n_{\uparrow}, n_{\downarrow}] - \sum_{\sigma=\{\uparrow,\downarrow\}} N_{\sigma} (E_{\text{H}}[n_{\sigma}/N_{\sigma}] + E_{xc}^{\text{DFT}}[n_{\sigma}/N_{\sigma}, 0]). \quad (10)$$

Following this logic, one could be tempted to average not the up and down densities of collinear SDFT, but the full spin-density matrix of non-collinear SDFT or, equivalently, the local charge and magnetization densities. Inserting this into Eq. (9), one would directly obtain

$$E_{xc}^{\text{AD-SIC}} = E_{xc}^{\text{DFT}}[n, \mathbf{m}] - N (E_{\text{H}}[n/N] + E_{xc}^{\text{DFT}}[n/N, \mathbf{m}/N]). \quad (11)$$

However, this choice does not produce the correct collinear limit. In order to illustrate this, let us consider a Li atom in a uniform

magnetic field aligned along the z direction. In this case, the system has three electrons, two residing at the $1s$ level and one at the $2s$ level. It is straightforward to see that the one electron in the $1s$ (spin-channel α) and the one in the $2s$ level have their orbital magnetization antialigned with the external magnetic field, while the second $1s$ electron (spin-channel β) has its orbital magnetization aligned with the external magnetization. The densities corresponding to these states are denoted $n_{1s,\alpha}$, $n_{2s,\alpha}$, and $n_{1s,\beta}$. Assuming that the approximate functional that we want to be corrected with AD-SIC fulfills the requirements mentioned in the introduction [SU(2) gauge invariance, the same energy for a single orbital density with $m_z > 0$ in the noncollinear case, and the same density in the up channel for the collinear functional], we can treat the same Li atom as a collinear electronic system with a static magnetic field along the z axis.

Let us now compute the collinear and noncollinear AD-SIC corrections for this Li atom. The AD-SIC for the collinear-spin case, Eq. (10), is

$$\Delta E^{\text{AD-SIC-coll.}} = -2E_{\text{H}} \left[\frac{n_{1s,\alpha} + n_{2s,\alpha}}{2} \right] - E_{\text{H}}[n_{1s,\beta}] - 2E_{\text{xc}} \left[\frac{n_{1s,\alpha} + n_{2s,\alpha}}{2}, 0 \right] - E_{\text{xc}}[n_{1s,\beta}, 0]. \quad (12)$$

If we use the proposed averaged density SIC, as in Eq. (11), we get

$$\Delta E_{\text{xc}}^{\text{AD-SIC}} = -3 \left(E_{\text{H}} \left[\frac{n_{1s,\alpha} + n_{2s,\alpha} + n_{1s,\beta}}{3} \right] + E_{\text{xc}}^{\text{DFT}} \left[\frac{n_{1s,\alpha} + n_{2s,\alpha} + n_{1s,\beta}}{3} \right] \times \frac{\mathbf{m}_{1s,\alpha} + \mathbf{m}_{2s,\alpha} + \mathbf{m}_{1s,\beta}}{3} \right). \quad (13)$$

Clearly, this expression will not lead to the desired collinear limit, as seen directly from the Hartree term. However, it is possible to recover the collinear limit using the same logic as originally proposed by Kübler *et al.*²³ for treating LSDA with noncollinear spin. By diagonalizing first the spin-density matrix, we obtain two densities, n_{\uparrow} and n_{\downarrow} , which we can average by normalizing them by their integrals (thus defining the number of “up” and “down” electrons in the frame defined by the local magnetization). Similarly to the LSDA case, the potential is computed in the local frame and independently for the up and down channels, and then rotated back to the global frame using the total magnetization. This procedure will produce the collinear limit expected in the above Li atom example.

The direct consequence of this procedure is that both the LSDA energy/potential and the AD-SIC corrections are evaluated in the same frame, which makes this approach consistent and also invariant under local and global SU(2) rotations. However, the price to pay is that the exchange-correlation magnetic field originating from the AD-SIC correction term is aligned with the local magnetization, meaning that no exchange-correlation torque is produced by the correction scheme.

III. NUMERICAL RESULTS

We have implemented the above-mentioned equations in the real-space code Octopus³⁴ in order to perform tests. For the case of PZ-SIC, we only computed the solution of the OEP equations at the

KLI level, using the explicit solution for noncollinear spin proposed in our recent work (see supplementary information in Ref. 22). All our SIC calculations are performed self-consistently.

A. Isolated Xe atom

In order to investigate the interplay between SIC and SOC, as well as numerical and theoretical problems related to the various schemes, we first consider the case of an isolated Xe atom. We use a grid spacing of 0.30 Bohr,³⁵ employing norm-conserving fully relativistic Hartwigsen–Goedecker–Hutter (HGH) pseudo-potentials.³⁶ The simulation box is taken as a sphere of radius 12 Bohr, centered at the atomic center. In Fig. 1, we show the splitting of the $5p$ electronic levels into $5p_{1/2}$ and $5p_{3/2}$ levels for LSDA, LSDA + AD-SIC, and LSDA + PZ-SIC. In all cases, the collinear limit is correctly recovered for PZ-SIC and AD-SIC. We found that the inclusion of the SIC does not change how SOC affects the energy levels, and the degeneracy of the energy levels is properly described by our corrections. As visible from the figure, we nicely recover the collinear limit, indicated by the symbols in Fig. 1. We also checked that in the case of vanishing SOC strength, using a small magnetic field along x , y , or z directions produces identical results, as expected from the SU(2) invariance of our proposed formulation. However, we note that for more complicated molecules, the collinear limit is not always recovered (see below).

Let us now comment on the dependence on a unitary transformation of the orbitals used in the evaluation of Eqs. (8) and (9). In order to reveal this, we define a new set of orbitals, $\{\tilde{\varphi}_i\}$, such that

$$\tilde{\varphi}_i(\mathbf{r}) = \sum_j U_{ij} \varphi_j(\mathbf{r}), \quad (14)$$

where U is a unitary matrix. The two sets of orbitals, $\{\varphi_j\}$ and $\{\tilde{\varphi}_i\}$, have the same density, but their contribution to their PZ-SIC energy is different. To illustrate this, we consider the following three cases: (i) the canonical orbitals obtained directly from the solution of the Kohn–Sham equations; (ii) the so-called subspace diagonalization

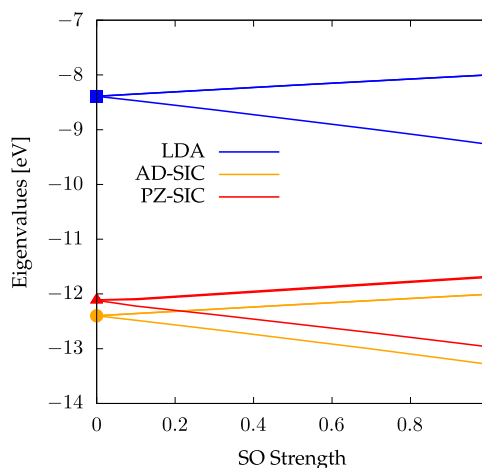


FIG. 1. Splitting of $5p$ levels of Xe due to SOC vs the spin–orbit strength computed for LDA (blue curves), LDA + AD-SIC (orange curves), and LDA + PZ-SIC (red curves). The symbols (square, circle, and triangle) indicate the results obtained for the corresponding spin-unpolarized calculations.

TABLE I. Total energy E_{tot} and ionization potential I_p , in Hartree, for the collinear and noncollinear cases using different orbitals, as explained in the main text.

	Collinear case		Noncollinear case	
	Canonical	SCDM	Canonical	SCDM
E_{tot}	-15.5938	-15.6492	-15.5938	-15.6499
I_p	0.4449	0.4674	0.4449	0.4695

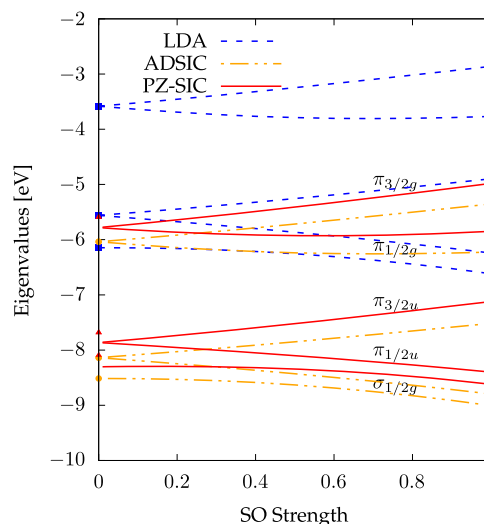
procedure in which the unitary matrix is found by diagonalizing the Hamiltonian matrix in the subspace of the canonical orbitals (a standard technique³⁷ for reducing the computational cost of iterating the Kohn–Sham equations); (iii) the localization method known as the SCDM³⁸ that produces Wannier functions by direct construction from a set of selected columns of the density matrix.

In Table I, we report the total energy and ionization potential of Xe for the first and last approaches for both the collinear and noncollinear cases. Here and in the following, the ionization potential is obtained from the eigenvalues and not from the difference of total energies. We find no difference between the canonical orbitals and the ones obtained by subspace diagonalization. As expected, more localized orbitals produce lower total energy and a higher ionization potential.

Overall, it is apparent from these results that our noncollinear functional suffers from the same problems as the collinear formulation. One solution would be to implement a minimization of the PZ-SIC energy correction with respect to the unitary transformation U , which we defer to some future work. In the following, unless specified explicitly, orbitals from the subspace diagonalization are always employed.

B. Diatomic closed-shell systems

We continue analyzing the effect of our proposed functional on small closed-shell molecules, for which SOC is known to be important for their electronic structure. It is known that SOC plays an important role in the bond length of closed-shell dimers, as well as their harmonic frequency and their dissociation energy.³⁹ However, the choice of the functional is also important for these properties,³⁹

**FIG. 2.** Eigenvalues of the highest bonding ($\sigma_{1/2g}$, $\pi_{1/2u}$, and $\pi_{3/2u}$) and lowest antibonding ($\pi_{1/2g}$ and $\pi_{3/2g}$) molecular orbitals of the bismuth dimer as a function of the SOC strength computed for LDA (blue curves), LDA + AD-SIC (orange curves), and LDA + PZ-SIC (red curves). The dots indicate the results obtained for spin-unpolarized calculations.

and we expect the SIC to be relevant for improving the theoretical modeling of these molecules.

We start by considering the Bi_2 molecule. We performed calculations at the experimental bond length⁴⁰ of 2.661 Å for LSDA, LSDA + AD-SIC, and LSDA + PZ-SIC. We used a grid spacing of 0.30 Bohr, employing norm-conserving fully relativistic Hartwigsen–Goedecker–Hutter (HGH) pseudo-potentials.³⁶ The simulation box was obtained from the union of two spheres of radius 12 Bohr centered on each atom. As shown in Fig. 2, the inclusion of the SIC does not change how SOC affects the energy levels of the molecules, and the degeneracy of the energy levels is properly described by our corrections.

As in the case of Xe, the AD-SIC properly recovers the collinear limit, while we found that the PZ-SIC does not converge when the

TABLE II. Ionization potentials, in eV, of diatomic systems using their experimental geometry, including SOC, for different energy functionals.

	Bi_2	Au_2	I_2	HI	IF	PbO	TlF
Exp.	7.3 ^a	9.5 ^b	9.307 ^c	10.386 ^d	10.54 ^e	9.4 ^f	10.52 ^g
LSDA	4.898	6.104	6.062	6.627	6.549	6.373	5.959
LSDA + AD-SIC	7.773	9.481	8.651	10.294	10.015	10.190	10.614
LSDA + PZ-SIC	7.120	9.324	8.252	10.028	9.481	10.372	11.778

^aReference 41.^bReference 42.^cReference 43.^dReference 44.^eReference 45.^fReference 46.^gReference 47.

SOC strength is set to zero. Indeed, in this case, Bi_2 is non-magnetic, and hence, any local $\text{SU}(2)$ rotation of the spins associated with a given orbital leaves the energy unchanged but changes the potential. In order to get a converged ground state in the absence of SOC, we apply a tiny magnetic field (of magnitude 10^{-3} a.u.). Unlike the case of Xe, we found here two possible solutions. By aligning the external magnetic field along the molecular axis, we get the limit of vanishing SOC strength. Aligning the magnetic field perpendicular to the molecular axis, we get the same eigenvalues as in the collinear calculation. This is analyzed more in detail in [Appendix A](#).

We also performed similar simulations for other diatomic molecules using their experimental geometry (see [Table II](#)). For all molecules, we employ a grid spacing of 0.3 Bohr and a radius for atom-center spheres of 12 Bohr, except for Au_2 , for which we included semi-core states and used a grid spacing of 0.25 Bohr. Overall, we find that the inclusion of the SIC drastically improves the agreement with respect to the experiment for the ionization potential, as expected from the vast literature on collinear SIC.

We also investigated the polar diatomic molecules HI, IF, PbO, and TlF at their experimental geometry and compared the dipole moments for different levels of description with the experimental values [Table III](#). We used here a grid spacing of 0.2 Bohr to ensure convergence of the dipole moments with respect to the grid spacing. Consistent with the collinear case,⁴⁸ we found that the dipole moment on average deviates more from the experimental value when using SIC than simply using noncollinear LSDA. Importantly, the limitations of the approximation of an averaged density used to get to AD-SIC appear more clearly on the dipole moments than on the ionization energy. We also performed geometry relaxation. As found in the collinear case,^{26,49,50} we obtain that including PZ-SIC and AD-SIC shortens the bonds, resulting in underestimated bond lengths compared to the LSDA, the latter being in better agreement with experimental values. However, one should note that this problem affects PZ-SIC and related approaches and, as shown in [Ref. 50](#), other SIC methods such as the locally scaled SIC can lead to improved bond lengths compared to LSDA.

C. Magnetic cluster

We now investigate the effect of SIC on the properties of small magnetic clusters by specifically considering the iron dimer, Fe_2 (see [Table IV](#)).⁵¹ Clusters of this type have been widely studied by means of LSDA, including SOC (see, for instance, [Ref. 52](#) and references therein). Unless stated differently, SOC is included throughout. In all calculations, we employ a grid spacing of 0.15 Bohr, a radius for atom-center spheres of 12 Bohr, and we include the semi-core states

TABLE III. Dipole moments, in Debye, of diatomic systems using their experimental geometry, including SOC, for different energy functionals.

	HI	IF	PbO	TlF
Exp. ^a	0.45	1.95	4.64	4.23
LSDA	0.466	1.768	4.508	4.032
LSDA + AD-SIC	0.549	2.905	6.446	5.984
LSDA + PZ-SIC	0.389	1.960	5.893	4.376

^aReference 40.

TABLE IV. Electronic and magnetic properties of Fe_2 for different energy functionals. Ionization potential (I_p) is given in eV, and the total (M) and atomic magnetic moments ($|\mathbf{m}|$) are given in μ_B and are obtained by integrating the density on a sphere of radius 1.909 Bohr around the atoms. Exchange-only LSDA (LSDAx) results were also reported.

	I_p	M	$ \mathbf{m} $
LSDA	3.327	6.00	2.71
LSDA + AD-SIC	7.854	6.00	2.69
LSDA + PZ-SIC	6.843	6.00	2.59
LSDAx	3.453	8.00	3.29
LSDAx + AD-SIC	7.464	7.00	2.97
LSDAx + PZ-SIC	5.995	7.50	3.10
Slater	6.760	6.00	2.96

for Fe atoms. A small Fermi–Dirac smearing of 10 meV for the occupations was also used. The Fe–Fe distance was taken for the Fe dimer to be the experimental one of 2.02 Å.⁵³

In all cases that included both LSDA exchange and correlation energy, we found a total magnetic moment of $6\mu_B$, in agreement with prior works. We note that our LSDA value matches well with the atomic magnetic moment reported in the pioneering work of Oda *et al.*⁵⁴ The fact that the atomic magnetic moments computed on a sphere around the atoms decrease indicates that for Fe_2 , the SIC tends to push away the magnetization from the atomic center, while the increase of the ionization potential is consistent with an increased localization of the orbitals. This points toward a non-negligible contribution of itinerant electrons to the magnetic properties of this cluster. We also computed the values for exchange-only LSDA, together with SIC corrections. The total magnetic moments are not properly predicted in these cases, demonstrating the key importance of correlations in order to obtain reliable magnetic structures.

We finally turn our attention to the exchange-correlation torque $\tau(\mathbf{r})$, defined as

$$\tau(\mathbf{r}) = \mathbf{m}(\mathbf{r}) \times \mathbf{B}_{\text{xc}}(\mathbf{r}), \quad (15)$$

where \mathbf{m} is the local magnetization density and \mathbf{B}_{xc} is the exchange-correlation magnetic field. We computed this quantity using LSDA and LSDAx with PZ-SIC and also with the Slater potential. As a reference here, we consider the Slater potential, which was shown to give reasonable results compared to the result of the exact-exchange potential computed at the level of KLI.²² From our results (see [Figs. 3\(a\)](#) and [3\(d\)](#)), the Slater potential produces a small exchange-correlation torque around the atoms, where the symmetries of the system are clearly apparent. Our results for PZ-SIC [[Figs. 3\(b\)](#), [3\(c\)](#), [3\(e\)](#), and [3\(f\)](#)] show that PZ-SIC also produces a non-vanishing torque around the atoms. While it shows, as required by the zero-torque theorem, alternating positive and negative patterns that are also in accordance with the symmetries of the system, the overall shape and magnitude strongly differ from what is obtained from Slater potential.

This qualitative difference in the exchange-correlation torques may be due to subtle phase effects. PZ-SIC and Slater both are orbital functionals, but PZ-SIC depends on orbital densities (where the orbital phases cancel out) and Slater depends on the one-body

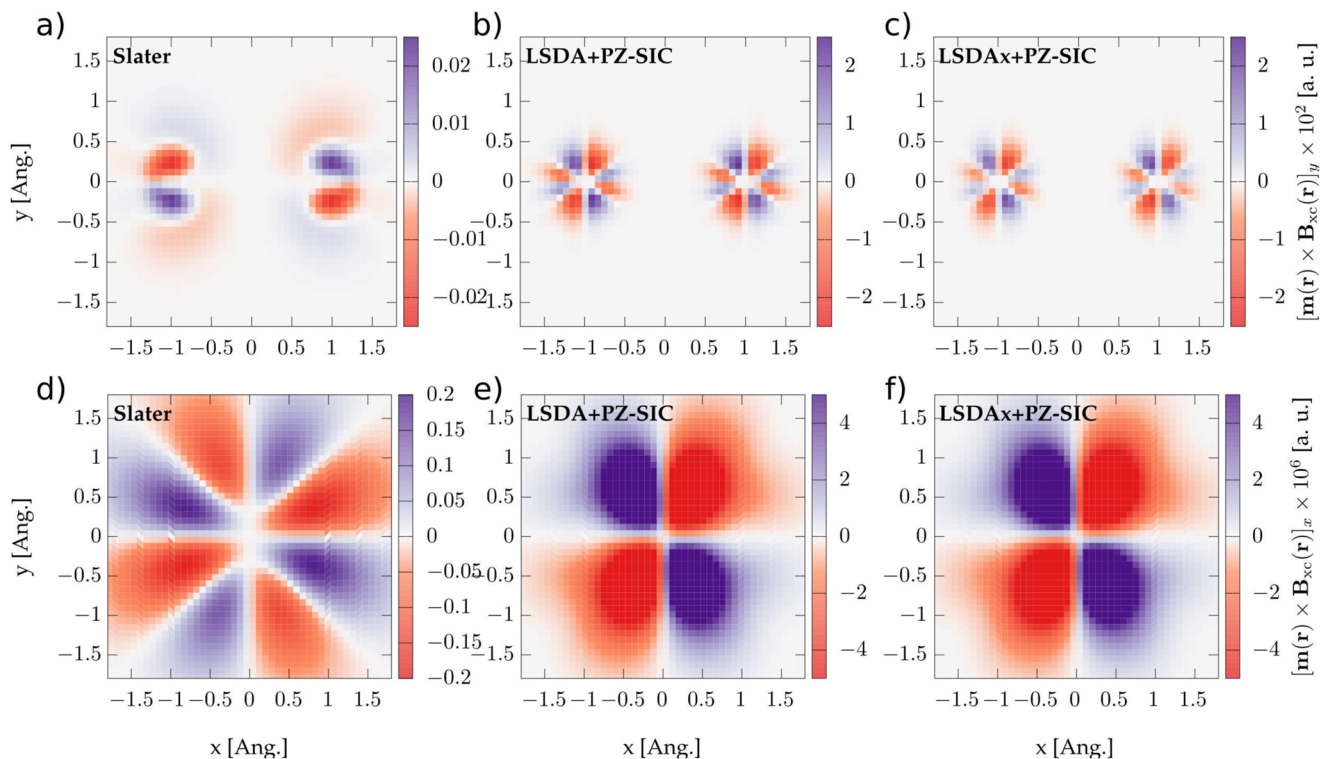


FIG. 3. Exchange torque for Fe_2 . Top panels: The y component of the local exchange torque $\tau(\mathbf{r})$ in the plane $y = 0$, computed from (a) Slater, (b) LSDA with PZ-SIC, and (c) LSDAx with PZ-SIC. Bottom panels: the same as the top panels, but showing the x component of the torque in the $z = 0$ plane.

reduced density matrix (where they do not). This suggests that the torques depend sensitively on the phase information of the orbitals, which would be an interesting subject for future investigation.

Importantly, we want to stress here that, like energy, the torque obtained from PZ-SIC depends upon the unitary transformation of the orbitals. This quantity, therefore, needs to be analyzed with great care, and we aim in the future at implementing a minimization over unitary transformations in order to eliminate this ambiguity, similar to prior efforts.³¹

IV. CONCLUSIONS

To summarize, we presented how to extend some of the existing SIC approaches to the case of non-collinear spins. We then analyzed numerically how these non-collinear SIC schemes behave for various closed-shell and magnetic systems. Overall, we found that our noncollinear schemes exhibit similar advantages and deficiencies as the collinear ones. The ionization energies are improved, but bond lengths are found to be worse than those obtained for LSDA. When the localization of individual orbitals is important, the AD-SIC performs poorly for observables that depend on local orbitals, like dipole moments or magnetic moments.

We further demonstrated that PZ-SIC for a noncollinear spin can produce a non-negligible exchange-correlation torque around the magnetic atoms, but we found large differences in the magnitude and texture of the exchange-correlation torque compared to the result of the Slater potential.

Overall, our work opens the door to a better description of the electronic and magnetic properties of systems when noncollinear effects are important, but we note that some further work, including the computation of accurate benchmarks, is needed in order to get reliable results for the collinear and noncollinear PZ-SIC schemes. Once such SIC schemes are fully established, we expect them to become a useful tool for the description of materials with noncollinear magnetism.

ACKNOWLEDGMENTS

C.A.U. is supported by DOE Grant No. DE-SC0019109.

AUTHOR DECLARATIONS

Conflict of Interest

The authors have no conflicts to disclose.

Author Contributions

Nicolas Tancogne-Dejean: Conceptualization (equal); Formal analysis (equal); Software (equal); Writing – original draft (equal); Writing – review & editing (equal). **Martin Lüders:** Conceptualization (equal); Writing – review & editing (equal). **Carsten**

A. Ullrich: Conceptualization (equal); Formal analysis (equal); Writing – original draft (equal); Writing – review & editing (equal).

DATA AVAILABILITY

The data that support the findings of this study are available from the corresponding author upon reasonable request.

APPENDIX: VANISHING SOC LIMIT IN Bi_2

In this section, we investigate in more detail the case of Bi_2 without SOC using PZ-SIC, with a tiny magnetic field included. As explained in the main text, the dependence on the orbitals leads to different results for a magnetic field aligned with the molecular axis as opposed to one aligned perpendicular to it. In Fig. 4, we report the square modulus of the four highest occupied states of Bi_2 computed with PZ-SIC, corresponding to the $\pi_{1/2u}$ and $\pi_{3/2u}$ bonding orbitals, without SOC, and with a magnetic field aligned with the molecular axis or perpendicular to it. While these orbitals produce the same

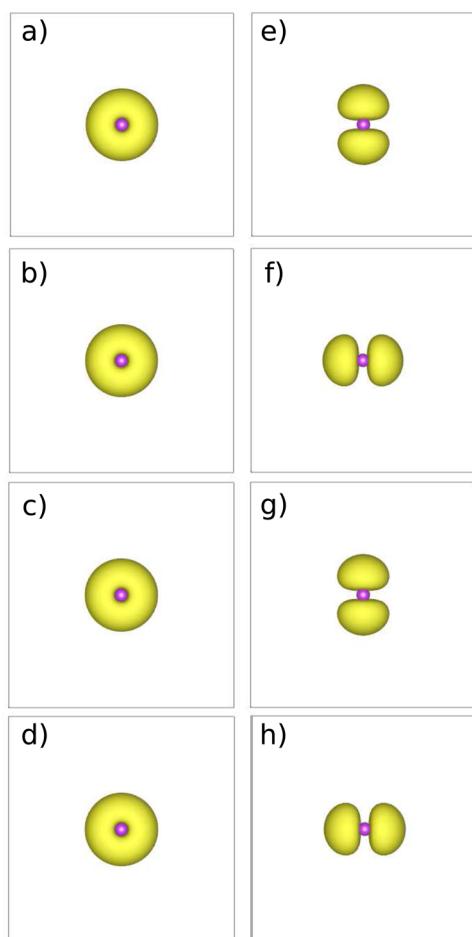


FIG. 4. Square modulus of the four highest occupied π_u orbitals of Bi_2 obtained for a magnetic field aligned with the molecular axis (a)–(d) or perpendicular to it (e)–(h). The plane shown in the figures is the plane perpendicular to the molecular axis.

charge density when summed over, their individual contributions to the PZ-SIC energy and potential are different, leading to a different ground state.

While these results might be surprising at first glance, the reported shapes are in fact the direct consequence of the symmetries of the system. When the system has a magnetic field aligned with the molecular axis, it is clear that the system is invariant under any rotation along this axis. It is, therefore, not surprising to find radially symmetric wavefunctions in the panels (a)–(d). On the contrary, when a tiny magnetic field is applied perpendicular to the molecular axis, the radial symmetry is broken, resulting in the splitting of the orbitals into two sets, one aligned with the magnetic field (e); (g) and one perpendicular to it (f); (h).

The obtained wavefunctions, therefore, respect the symmetries of the system in the presence of a tiny magnetic field, and it is, therefore, expected that taking these orbitals directly to build the PZ-SIC energy (and the potential following from it) leads to some differences,⁵⁵ even if the magnetic field itself has a negligible effect on the charge density. Importantly, the change in the orbitals leads to a large change of 35 mH in the total energy (the molecular-axis-aligned magnetic field giving the lowest energy), while the magnetic field itself only causes a splitting of these four energy levels by $15\mu\text{H}$.

REFERENCES

- 1 J. P. Perdew, "Climbing the ladder of density functional approximations," *MRS Bull.* **38**, 743 (2013).
- 2 J. P. Perdew and A. Zunger, "Self-interaction correction to density-functional approximations for many-electron systems," *Phys. Rev. B* **23**, 5048–5079 (1981).
- 3 A. J. Cohen, P. Mori-Sánchez, and W. Yang, "Challenges for density functional theory," *Chem. Rev.* **112**, 289 (2012).
- 4 I. Lindgren, "A statistical exchange approximation for localized electrons," *Int. J. Quantum Chem.* **5**, 411–420 (2009).
- 5 A. Seidl, A. Görling, P. Vogl, J. A. Majewski, and M. Levy, "Generalized Kohn-Sham schemes and the band-gap problem," *Phys. Rev. B* **53**, 3764–3774 (1996).
- 6 J. D. Talman and W. F. Shadwick, "Optimized effective atomic central potential," *Phys. Rev. A* **14**, 36 (1976).
- 7 D. Vieira, K. Capelle, and C. A. Ullrich, "Physical signatures of discontinuities of the time-dependent exchange-correlation potential," *Phys. Chem. Chem. Phys.* **11**, 4647 (2009).
- 8 S. Kümmel and L. Kronik, "Orbital-dependent density functionals: Theory and applications," *Rev. Mod. Phys.* **80**, 3–60 (2008).
- 9 Z.-h. Yang, H. Peng, J. Sun, and J. P. Perdew, "More realistic band gaps from meta-generalized gradient approximations: Only in a generalized Kohn-Sham scheme," *Phys. Rev. B* **93**, 205205 (2016).
- 10 J. B. Krieger, Y. Li, and G. J. Iafrate, "Construction and application of an accurate local spin-polarized Kohn-Sham potential with integer discontinuity: Exchange-only theory," *Phys. Rev. A* **45**, 101–126 (1992).
- 11 M. F. Politis, P. A. Hervieux, J. Hanssen, M. E. Madjet, and F. Martín, "Electron capture and excitation in proton- Na_{20} collisions at low velocities," *Phys. Rev. A* **58**, 367–376 (1998).
- 12 C. A. Ullrich, P.-G. Reinhard, and E. Suraud, "Simplified implementation of self-interaction correction in sodium clusters," *Phys. Rev. A* **62**, 053202 (2000).
- 13 C. Legrand, E. Suraud, and P. Reinhard, "Comparison of self-interaction-corrections for metal clusters," *J. Phys. B: At., Mol. Opt. Phys.* **35**, 1115 (2002).
- 14 R. R. Zope, Y. Yamamoto, C. M. Diaz, T. Baruah, J. E. Peralta, K. A. Jackson, B. Santra, and J. P. Perdew, "A step in the direction of resolving the paradox of Perdew-Zunger self-interaction correction," *J. Chem. Phys.* **151**, 214108 (2019).
- 15 S. Yamanaka, D. Yamaki, S. Kiribayashi, and K. Yamaguchi, "Generalized spin density functional theory for noncollinear molecular magnetism II—Influence of

- gradient correction and self-interaction correction," *Int. J. Quantum Chem.* **85**, 421–431 (2001).
- ¹⁶O. Gunnarsson and B. I. Lundqvist, "Exchange and correlation in atoms, molecules, and solids by the spin-density-functional formalism," *Phys. Rev. B* **13**, 4274–4298 (1976).
- ¹⁷K. Capelle, G. Vignale, and C. A. Ullrich, "Spin gaps and spin-flip energies in density-functional theory," *Phys. Rev. B* **81**, 125114 (2010).
- ¹⁸C. A. Ullrich, "Density-functional theory for systems with noncollinear spin: Orbital-dependent exchange-correlation functionals and their application to the Hubbard dimer," *Phys. Rev. B* **98**, 035140 (2018).
- ¹⁹E. A. Pluhar and C. A. Ullrich, "Exchange-correlation magnetic fields in spin-density-functional theory," *Phys. Rev. B* **100**, 125135 (2019).
- ²⁰D. Hill, J. Shotton, and C. A. Ullrich, "Magnetization dynamics with time-dependent spin-density functional theory: Significance of exchange-correlation torques," *Phys. Rev. B* **107**, 115134 (2023).
- ²¹K. Capelle, G. Vignale, and B. L. Györfy, "Spin currents and spin dynamics in time-dependent density-functional theory," *Phys. Rev. Lett.* **87**, 206403 (2001).
- ²²N. Tancogne-Dejean, A. Rubio, and C. A. Ullrich, "Constructing semilocal approximations for noncollinear spin density functional theory featuring exchange-correlation torques," *Phys. Rev. B* **107**, 165111 (2023).
- ²³J. Kübler, K.-H. Höck, J. Sticht, and A. Williams, "Density functional theory of non-collinear magnetism," *J. Phys. F: Met. Phys.* **18**, 469 (1988).
- ²⁴S. Pittalis, G. Vignale, and F. G. Eich, "U(1) × SU(2) gauge invariance made simple for density functional approximations," *Phys. Rev. B* **96**, 035141 (2017).
- ²⁵A. D. Becke and M. R. Roussel, "Exchange holes in inhomogeneous systems: A coordinate-space model," *Phys. Rev. A* **39**, 3761–3767 (1989).
- ²⁶S. Goedecker and C. J. Umrigar, "Critical assessment of the self-interaction-corrected-local-density-functional method and its algorithmic implementation," *Phys. Rev. A* **55**, 1765–1771 (1997).
- ²⁷R. A. Heaton, J. G. Harrison, and C. C. Lin, "Self-interaction correction for density-functional theory of electronic energy bands of solids," *Phys. Rev. B* **28**, 5992–6007 (1983).
- ²⁸M. R. Pederson, R. A. Heaton, and C. C. Lin, "Local-density Hartree-Fock theory of electronic states of molecules with self-interaction correction," *J. Chem. Phys.* **80**, 1972–1975 (1984).
- ²⁹M. R. Pederson, R. A. Heaton, and C. C. Lin, "Density-functional theory with self-interaction correction: Application to the lithium molecule," *J. Chem. Phys.* **82**, 2688–2699 (1985).
- ³⁰M. R. Pederson and C. C. Lin, "Localized and canonical atomic orbitals in self-interaction corrected local density functional approximation," *J. Chem. Phys.* **88**, 1807–1817 (1988).
- ³¹S. Lehtola and H. Jónsson, "Correction to variational, self-consistent implementation of the Perdew-Zunger self-interaction correction with complex optimal orbitals," *J. Chem. Theory Comput.* **11**, 5052–5053 (2015).
- ³²M. R. Pederson, A. Ruzsinszky, and J. P. Perdew, "Communication: Self-interaction correction with unitary invariance in density functional theory," *J. Chem. Phys.* **140**, 121103 (2014).
- ³³P. Klüpfel, P. M. Dinh, P.-G. Reinhard, and E. Suraud, "Koopmans' condition in self-interaction-corrected density-functional theory," *Phys. Rev. A* **88**, 052501 (2013).
- ³⁴N. Tancogne-Dejean, M. J. T. Oliveira, X. Andrade, H. Appel, C. H. Borca, G. Le Breton, F. Buchholz, A. Castro, S. Corni, A. A. Correa, U. De Giovannini, A. Delgado, F. G. Eich, J. Flick, G. Gil, A. Gomez, N. Helbig, H. Hübener, R. Jestädt, J. Jorner-Somoza, A. H. Larsen, I. V. Lebedeva, M. Lüders, M. A. L. Marques, S. T. Ohlmann, S. Pipolo, M. Rampp, C. A. Rozzi, D. A. Strubbe, S. A. Sato, C. Schäfer, I. Theophilou, A. Welden, and A. Rubio, "Octopus, a computational framework for exploring light-driven phenomena and quantum dynamics in extended and finite systems," *J. Chem. Phys.* **152**, 124119 (2020).
- ³⁵Here and in the following, the grid spacing is chosen by the requirement that the energy is converged to within 1 mHa.
- ³⁶C. Hartwigsen, S. Goedecker, and J. Hutter, "Relativistic separable dual-space Gaussian pseudopotentials from H to Rn," *Phys. Rev. B* **58**, 3641–3662 (1998).
- ³⁷S. Khadatkar and P. Motamarri, "Subspace recursive Fermi-operator expansion strategies for large-scale DFT eigenvalue problems on HPC architectures," *J. Chem. Phys.* **159**, 031102 (2023).
- ³⁸A. Damle, L. Lin, and L. Ying, "Compressed representation of Kohn-Sham orbitals via selected columns of the density matrix," *J. Chem. Theory Comput.* **11**, 1463–1469 (2015).
- ³⁹E. van Lenthe, J. Snijders, and E. Baerends, "The zero-order regular approximation for relativistic effects: The effect of spin-orbit coupling in closed shell molecules," *J. Chem. Phys.* **105**, 6505–6516 (1996).
- ⁴⁰K.-P. Huber, "Constants of diatomic molecules," *Mol. Spectra Mol. Struct.* **4**, 146–291 (1979).
- ⁴¹K. Gingerich, D. Cocke, and J. Kordis, "Gaseous phosphorus compounds. X. Mass spectrometric determination of the dissociation energies of arsenic and bismuth monophosphides," *J. Phys. Chem.* **78**, 603–606 (1974).
- ⁴²C. A. Stearns and F. J. Kohl, "Mass spectrometric determination of the dissociation energies of AlC₂, Al₂C₂, and AlAuC₂," *J. Phys. Chem.* **77**, 136–138 (1973).
- ⁴³M. Cockett, R. Donovan, and K. Lawley, "Zero kinetic energy pulsed field ionization (ZEKE-PFI) spectroscopy of electronically and vibrationally excited states of I₂⁺: The A²Π_{3/2,u} state and a new electronic state, the a⁴Σ_u⁻ state," *J. Chem. Phys.* **105**, 3347–3360 (1996).
- ⁴⁴J. Eland and J. Berkowitz, "Photoionization mass spectrometry of HI and DI at high resolution," *J. Chem. Phys.* **67**, 5034–5039 (1977).
- ⁴⁵E. Colbourn, J. Dyke, N. Fayad, and A. Morris, "The He(I) photoelectron spectra of BrF and IF," *J. Electron Spectrosc. Relat. Phenom.* **14**, 443–452 (1978).
- ⁴⁶A. Makarov and S. Zvezhneva, "Use of high-temperature mass spectrometry for vapor phase analysis of some materials used in film deposition technology," *Vysokochist. Veshchestva* **1**, 124–128 (1993).
- ⁴⁷J. L. Dehmer, J. Berkowitz, and L. Cusachs, "Photoelectron spectroscopy of high-temperature vapors. III. Monomer and dimer spectra of thallos fluoride," *J. Chem. Phys.* **58**, 5681–5686 (1973).
- ⁴⁸S. Adhikari, B. Santra, S. Ruan, P. Bhattarai, N. K. Nepal, K. A. Jackson, and A. Ruzsinszky, "The Fermi-Löwdin self-interaction correction for ionization energies of organic molecules," *J. Chem. Phys.* **153**, 184303 (2020).
- ⁴⁹A. I. Johnson, K. P. Withanage, K. Sharkas, Y. Yamamoto, T. Baruah, R. R. Zope, J. E. Peralta, and K. A. Jackson, "The effect of self-interaction error on electrostatic dipoles calculated using density functional theory," *J. Chem. Phys.* **151**, 174106 (2019).
- ⁵⁰Y. Yamamoto, T. Baruah, P.-H. Chang, S. Romero, and R. R. Zope, "Self-consistent implementation of locally scaled self-interaction-correction method," *J. Chem. Phys.* **158**, 064114 (2023).
- ⁵¹We also considered Fe₃, which led to similar conclusions as Fe₂, so the results are not shown here.
- ⁵²A. Aktürk and A. Sebetci, "BH-DFTB/DFT calculations for iron clusters," *AIP Adv.* **6**, 055103 (2016).
- ⁵³H. Purdum, P. A. Montano, G. K. Shenoy, and T. Morrison, "Extended-x-ray-absorption-fine-structure study of small Fe molecules isolated in solid neon," *Phys. Rev. B* **25**, 4412–4417 (1982).
- ⁵⁴T. Oda, A. Pasquarello, and R. Car, "Fully unconstrained approach to non-collinear magnetism: Application to small Fe clusters," *Phys. Rev. Lett.* **80**, 3622–3625 (1998).
- ⁵⁵C. Shahi, P. Bhattarai, K. Wagle, B. Santra, S. Schwalbe, T. Hahn, J. Kortus, K. A. Jackson, J. E. Peralta, K. Trepte, S. Lehtola, N. K. Nepal, H. Myneni, B. Neupane, S. Adhikari, A. Ruzsinszky, Y. Yamamoto, T. Baruah, R. R. Zope, and J. P. Perdew, "Stretched or noded orbital densities and self-interaction correction in density functional theory," *J. Chem. Phys.* **150**, 174102 (2019).